

# PD-L1 expression-related PI3K pathway correlates with immunotherapy efficacy in gastric cancer

Langbiao Liu\*, Lei Niu\*, Xue Zheng\*, Fei Xiao, Huaibo Sun, Wei Deng and Jun Cai 

Ther Adv Med Oncol

2023, Vol. 15: 1–14

DOI: 10.1177/  
17588359231205853

© The Author(s), 2023.  
Article reuse guidelines:  
sagepub.com/journals-  
permissions

## Abstract

**Background:** The programmed death ligand-1 combined positive score (PD-L1 CPS), the only FDA-approved biomarker for immune checkpoint inhibitor therapy in gastric cancer (GC) patients, is an important but imperfect predictive biomarker. The molecular characteristics of tumors that influence the PD-L1 CPS are largely unknown and would be helpful for screening patients who would benefit from immunotherapy.

**Methods:** PD-L1 immunohistochemistry (IHC) and targeted next-generation sequencing techniques were used to compare genomic alterations in 492 GC patients in two groups (PD-L1 CPS  $\geq 1$ , positive; CPS  $< 1$ , negative). Screened PD-L1 expression-related factors were analyzed for immunotherapy efficacy in three distinct GC cohorts from public databases.

**Results:** Positive PD-L1 expression occurred in 40% of GC patients and was associated with a higher proportion of phosphatidylinositol 3-kinase (PI3K), SWItch/Sucrose NonFermentable (SWI/SNF), lysine demethylase (KDM), and DNA (cytosine-5)-methyltransferase (DNMT) (all  $p < 0.01$ ), pathway alterations. Compared to wild-type GC patients, those with PI3K pathway alterations had a higher response rate ( $p = 0.002$ ) and durable clinical benefit rate with immunotherapy ( $p = 0.023$ ,  $p = 0.038$ ) as well as longer progression-free survival ( $p = 0.084$ ,  $p = 0.0076$ ) and overall survival ( $p = 0.2$ ,  $p = 0.037$ ) with immunotherapy.

**Conclusion:** This study revealed PD-L1 expression-related factors in the tumor genome in a GC cohort. Alterations in the PI3K pathway associated with PD-L1 positivity were shown to be associated with better immunotherapy efficacy in three distinct GC cohorts from public databases. Our results provide a potential avenue for patient selection and rational immune combination development for GC patients.

**Keywords:** CPS, gastric cancer, immunotherapy, PD-L1 expression, PI3K pathway

Received: 13 April 2023; revised manuscript accepted: 18 September 2023.

## Introduction

Immune checkpoint inhibitors (ICIs), primarily programmed death-1 (PD-1) inhibitors, have recently revolutionized treatment of gastric cancer (GC) and have emerged as a promising treatment strategy for GC patients. As the only Food and Drug Administration (FDA)-approved prediction biomarker for ICI therapy in patients with GC, the programmed death ligand-1 combined positive score (PD-L1 CPS) has some utility as a predictor of the efficacy of PD-1/PD-L1 inhibitors alone, but prediction of the efficacy of immunotherapy/

chemotherapy combinations varies among ICIs<sup>1–3</sup>; furthermore, the optimal threshold needs to be evaluated in clinical trials across treatment lines.<sup>2,4–8</sup> In salvage settings without selective biomarkers or PD-L1 expression, PD-1 inhibitors have a fairly wide range of response rates (10–26%) for metastatic GC.<sup>4,6,9</sup> More importantly, in clinical practice, multiple factors may interfere with PD-L1 assay results<sup>10</sup>; these include inter- and intratumor heterogeneity,<sup>11,12</sup> different detection antibodies and platforms,<sup>13</sup> strong subjectivity of different pathologists<sup>11</sup> and, as a continuous

Correspondence to:

**Jun Cai**

Beijing Key Laboratory of Cancer Invasion and Metastasis Research & National Clinical Research Center for Digestive Diseases, Department of General Surgery, Beijing Friendship Hospital, Capital Medical University, No. 95, Yong'an Road, Xicheng District, Beijing, 100050, China  
[juncain1@163.com](mailto:juncain1@163.com)

**Wei Deng**

Beijing Key Laboratory of Cancer Invasion and Metastasis Research & National Clinical Research Center for Digestive Diseases, Department of General Surgery, Beijing Friendship Hospital, Capital Medical University, No. 95, Yong'an Road, Xicheng District, Beijing 100050, China  
[dengweiwei@126.com](mailto:dengweiwei@126.com)

**Langbiao Liu**

**Lei Niu**

Beijing Key Laboratory of Cancer Invasion and Metastasis Research & National Clinical Research Center for Digestive Diseases, Department of General Surgery, Beijing Friendship Hospital, Capital Medical University, Beijing, China

**Xue Zheng**

**Fei Xiao**

**Huaibo Sun**

Genecast Biotechnology Co., Ltd, Wuxi City, Jiangsu, China

\*These authors contributed equally



variable, possible gray areas above and below the cutoff value. It is clear that PD-L1 expression is an important but imperfect predictive biomarker for treatment of GC with ICIs. Taken together, findings to date illustrate the importance of identifying other more effective predictive biomarkers associated with treatment of GC with ICIs.

In GC, most studies have focused mainly on the association of PD-L1 expression with specific molecular features, including MAPK pathway mutations, high microsatellite instability (MSI-H) and KMT2 gene mutations.<sup>14–18</sup> Furthermore, recent data indicate that specific molecular features may affect the predictive utility of PD-L1 expression.<sup>14,19</sup> Systematic exploration of the impact of clinical features and molecular features on PD-L1 expression has not been performed. Further clarification of the link between the PD-L1 CPS as well as clinical and molecular features may provide new insights into the search for predictive markers and rational drug combinations for GC immunotherapy.

In this study, we investigated the clinical features and genomic features of tumors in different PD-L1 CPS groups (CPS  $\geq$  1, < 1) in a cohort containing 492 GC patients (GC cohort) from the real world, with PD-L1 testing and targeted next-generation sequencing (NGS) performed on same tissue samples. Three GC cohorts treated with ICIs from Samsung Medical Center (SMC), Peking University Cancer Hospital (PUCH), and Memorial Sloan Kettering Cancer Center (MSK) were also used to evaluate how these molecular features may impact the efficacy of immunotherapy or prognosis in GC patients.

## Materials and methods

### Patient selection

*Patients from the GC cohort.* To characterize the relationship between both clinical features and molecular features and PD-L1 expression, we used a retrospective cohort of 492 patients with stage I-IV GC from April 2018 to December 2022. The main inclusion criteria of the GC cohort were as follows: (1) GC diagnosis, (2) complete basic clinical information, (3) available NGS and PD-L1 testing data, and (4) quality control carried out (Supplemental Figure 1).

*Patients from public databases.* The detailed patient selection process is presented in Supplemental

Figure 1. To analyze the association between specific PD-L1-related molecular features from the GC cohort and immunotherapy efficacy, we collected whole-exome sequencing (WES) data for 94 GC patients treated with ICIs from the SMC and PUCH immunotherapy cohorts. In the SMC immunotherapy cohort, a total of 49 GC patients treated with a PD-1 inhibitor were included in the final analysis after excluding two patients in whom the best response was not evaluated and four patients for whom there were no PD-L1 assay results. In the PUCH immunotherapy cohort, a total of 22 GC patients who were treated with only a PD-1 inhibitor were included in the final analysis (14 patients treated with PD-L1 inhibitors or immunocombination therapy and three who had no PD-L1 assay results were excluded). Single-nucleotide variants (SNVs) and insertions/deletions (indels) in the PUCH immunotherapy cohort were obtained from the figshare database (<https://figshare.com/>). Furthermore, a PD-1 immune checkpoint monotherapy cohort (MSK immunotherapy cohort) of 19 gastric or gastroesophageal junction adenocarcinoma patients with follow-up information was used to explore the correlation between specific molecular features and the efficacy and prognosis of ICI therapy. SNVs and indels of the MSK immunotherapy cohort were obtained from cBioPortal (<https://www.cbioportal.org/>). Fastq files of the SMC immunotherapy cohort were obtained from the European Nucleotide Archive (<https://www.ebi.ac.uk/>; Supplemental Table 1).

Tumor response was determined according to the Response Evaluation Criteria in Solid Tumors 1.1 (RECIST v1.1). In general, response (R) was defined as confirmed complete response (CR) or partial response (PR); nonresponse (NR) was defined as confirmed stable disease (SD) or progressive disease (PD).<sup>20</sup> Durable clinical benefit (DCB) was defined as CR, PR, or SD lasting 24 weeks; no durable benefit (NDB) was defined as progressive disease or SD lasting < 24 weeks.<sup>21</sup> Progression-free survival (PFS) and overall survival (OS) were defined as the time from the start of immunotherapy to the date of radiographic disease progression, death or last evaluation.<sup>21,22</sup> For basic demographic information on the GC, SMC, PUCH, and MSK immunotherapy cohorts, see Supplemental Table 2.

### PD-L1 immunohistochemistry

PD-L1 expression in the GC cohort was assessed using the combined positive score (CPS) and the

tumor percentage score (TPS) by IHC staining of formalin-fixed paraffin-embedded (FFPE) sections using an anti-PD-L1 antibody (clone 22C3, 1:50, Dako, M3653). As previously reported, the CPS was calculated as the number of PD-L1 positive cells (tumor cells, lymphocytes, and macrophages) divided by the total number of tumor cells multiplied by 100,<sup>23</sup> and the TPS was calculated according to the ratio of PD-L1-stained tumor cells to the total number of viable tumor cells.<sup>24</sup> PD-L1 positivity was defined as a CPS  $\geq$  1; PD-L1 negativity was defined as a CPS  $<$  1.

### *NGS of the GC cohort*

Genomic DNA from white blood cells and FFPE tumor tissue was extracted with TIANamp Genomic DNA Kit (TIANGEN, Beijing, China) and blackPREP FFPE DNA Kit (Analytic Jena, Germany), respectively. Genomic DNA was sheared into 150- to 200-bp fragments using a Covaris M220 according to the recommended settings. Fragmented DNA was input for library construction. A KAPA hyper preparation kit (Kapa Biosystems, Wilmington, USA) was used to prepare indexed Illumina NGS libraries according to the manufacturer's instructions. Nine polymerase chain reaction (PCR) cycles of ligated fragments were amplified using index primers according to the DNA quality of the pre-PCR. DNA was purified with Agencourt AMPure XP beads (Beckman-Coulter, CA, USA), and double size screening was performed for library preparation. All the libraries were quantified using a Qubit DNA dsDNA assay kit (Thermo Fisher, Massachusetts, USA), and fragment length was determined using a DNA 1000 kit (Agilent, CA, USA) on an Agilent Bioanalyzer 2100. The DNA libraries were sequenced using 150-bp paired-end runs with an Illumina NovaSeq 6000 and captured with two designed Genescope panels (Genecast, Beijing, China) including 414 shared tumor-related genes. For WES cohorts from public databases, only these 414 genes were included in the analysis. For the cohort of panel capture sequences from the public database, genes shared with these 414 genes were assessed.

### *Variant calling*

*Variant calling for the GC cohort.* For the GC cohort, the mean coverage depth after deduplication across all target regions on tissue samples and matched white blood cells was 2124 $\times$  and 495 $\times$ ,

respectively. The software programs VarDict (version 1.5.1; <https://github.com/AstraZeneca-NGS/VarDict>) and FreeBayes (version 1.2.0; <https://github.com/freebayes/freebayes>) were used to identify SNVs and indels in each patient's tumor tissues and matched white blood cells. Matched white blood cells from each patient were used to filter the germline variants, clonal hematopoiesis, and sequence artifacts to obtain somatic genetic alterations of tumor tissue. The ANNOVAR assay was used to annotate the function of genetic variants. Somatic genetic alterations, including SNVs and indels, were selected by the following exclusion criteria: (1) located in intergenic regions or intronic regions; (2) synonymous SNVs; (3) minor allele frequency (MAF)  $\geq$  0.002 in the Exome Aggregation Consortium (ExAC) and Genome Aggregation Database (gnomAD; <https://gnomad.broadinstitute.org/>); (4) variant allele frequency (VAF)  $<$  0.01 in tumor tissue; (5) strand bias for genetic alterations in the reads; (6) number of supporting reads for a variation  $<$  2; and (7) depth  $<$  30 $\times$ .<sup>25-31</sup> For copy number variation (CNV) calling, white blood cell samples of patients were used as a paired control, and the CONTRA assay (version 2.0.8) was used to call CNVs from the FFPE tumor samples for each patient with a copy number threshold of 3 for CNV gain and 1.2 for CNV loss.<sup>32</sup> CNV burden was determined as the total number of genes with copy number gains or losses.

*WES variant calling.* For the SMC immunotherapy cohort, our analysis started with data in the fastq file format. The average sequencing depths of tumor samples and normal samples after deduplication were 139 $\times$  and 92 $\times$ , respectively. After removing low-quality reads using fastp (version 0.23.1), clean reads were aligned to the human reference genome (Hg19, NCBI Build 37.5) with Burrows-Wheeler Aligner (version 0.7.17).<sup>33</sup> Then, the Picard toolkit (version 2.26.4; <http://broadinstitute.github.io/picard/>) was used to create duplicates, and Genome Analysis Tool Kit (GATK, version 4.2.2.0; <https://gatk.broadinstitute.org/>) was used for realignment.<sup>34</sup> The MuTect2 tool of Genome Analysis Tool Kit was used to call SNV and indel alterations in tumor and normal samples, and then the alterations were annotated through VEP (version 104.3).<sup>35</sup> Finally, somatic alterations were obtained after filtering germline alterations, and the final somatic alterations used for the following analysis were selected based on the following standards: (1) the

result of GATK filtering was PASS; (2) normal sample depth  $\geq 30\times$  and tumor sample depth  $\geq 50\times$ ; (3) number of supporting reads for an alteration was both  $\geq 5$  in tumor samples and  $\leq 3$  in control samples; (4) both tumor sample VAF  $\geq 0.03$  and (tumor sample VAF)/(normal sample VAF)  $\geq 5$ ; (5) MAF  $< 0.01$  in the databases ExAC and gnomAD; and (6) the Sorting Intolerant from Tolerant (SIFT) database<sup>36</sup> did not classify the alteration as tolerated, and the Polymorphism Phenotyping (PolyPhen) database did not classify the alteration as benign.<sup>37</sup>

*Analysis of the microsatellite instability status, tumor mutational burden, and mutant-allele tumor heterogeneity in the GC cohort*

**Microsatellite instability status assessment.** Microsatellites were defined as tandem DNA repeats with one to six bases in coding and noncoding regions throughout the genome. Microsatellite instability (MSI) is a hypermutable phenotype at the genomic level due to deficient mismatch repair (MMR) activity caused by germline mutations or gene hypermethylation in the DNA MMR system, which detects and corrects errors such as base–base mismatches and insertion–deletions in microsatellites caused by polymerase slippage during DNA synthesis.<sup>38</sup> For assessment of MSI status, the NGS method has shown good agreement with PCR or immunohistochemistry in several studies.<sup>39–41</sup> MSI status in the GC cohort was evaluated as follows.

Adaptors of raw read pairs were trimmed using Trimmomatic (version 0.39; <https://github.com/topics/trimmomatic>). Clean reads were mapped against the human reference genome (build hg19, UCSC) using Burrows-Wheeler-Alignment Tool (BWA, version 0.7.12; <https://bio-bwa.sourceforge.net/>) and sorted using SAMtools (version 1.3; <https://github.com/samtools/samtools>). Duplicates were performed followed by local indel realignment using GATK (version v2.8; <https://gatk.broadinstitute.org/>). For each microsatellite locus, all spanning reads (covering at least 2bp in both the 5' and 3' directions) were extracted from a realigned BAM file. Following deduplication, the length of the mononucleotide repeat in each deduped alignment was counted and tallied by length. The number of alleles of each observed length compared to the reference genome within each of the microsatellite loci for 30 healthy blood samples was evaluated, and then the mean and SD of the number of alleles were

calculated as the baseline reference value. Experimental results were compared against baseline reference values at each locus to assess the instability of microsatellite loci. If the tally of alleles counted exceeded the MSI stable reference value of [mean number of alleles + (3 × SD)], the locus was scored as lightly unstable. If the tally of alleles counted exceeded the MSI stable reference value of [mean number of alleles + (4 × SD)], the locus was scored as heavily unstable. Finally, the fraction of unstable loci among all loci analyzed was calculated for each experimental sample. A fraction of 25% lightly unstable loci or a fraction of 15% heavily unstable loci was considered to indicate MSI. The QC check was as follows: (1) microsatellite loci were covered by at least 100 spanning reads; (2) the duplication ratio of each microsatellite locus was  $\geq 30\%$ ; (3) each allele was covered by at least two spanning reads; and (4) alleles with  $< 5\%$  of the reads counted for the most frequently observed allele were excluded.

**Tumor mutational burden calculation.** Tumor mutational burden (TMB) was calculated as the number of somatic, coding, base substitutions, and short indels detected in each Mb genome.<sup>42</sup> In several clinical trials, TMB has been shown to be a good predictor of immunotherapy efficacy<sup>43,44</sup> and has emerged as a surrogate for neoantigen burden, which is an independent biomarker associated with the outcome of ICIs.<sup>45</sup> SNV mutations for TMB calculation were filtered through the following rules: (1) no splicing or exonic mutations; (2) depth  $< 100\times$  and VAF  $< 0.05$ ; (3) MAF  $\geq 0.002$  in the databases ExAC and gnomAD; and (4) strand bias mutations in the reads and other rules as previously reported.<sup>44</sup> Then, we calculated the TMB of the tumor samples after obtaining the absolute mutation counts of the tumor samples against the mutation spots of the normal samples with the following formula: absolute mutation counts  $\times 1000,000$ /panel exonic base number. The TMB was measured in mutations per Mb.

**Mutant-allele tumor heterogeneity calculation.** Mutant-allele tumor heterogeneity (MATH) is an algorithm to quantify the genetic heterogeneity of a tumor sample based on the mutant allele frequencies of all alleles in the tumor, and a MATH value is calculated for each sample, which reflects the level of tumor heterogeneity.<sup>46</sup> The VAF of the alteration was calculated as the ratio of alternate allele observations to the read depth at each position. We modified the MATH score to include all somatic variants with a VAF between

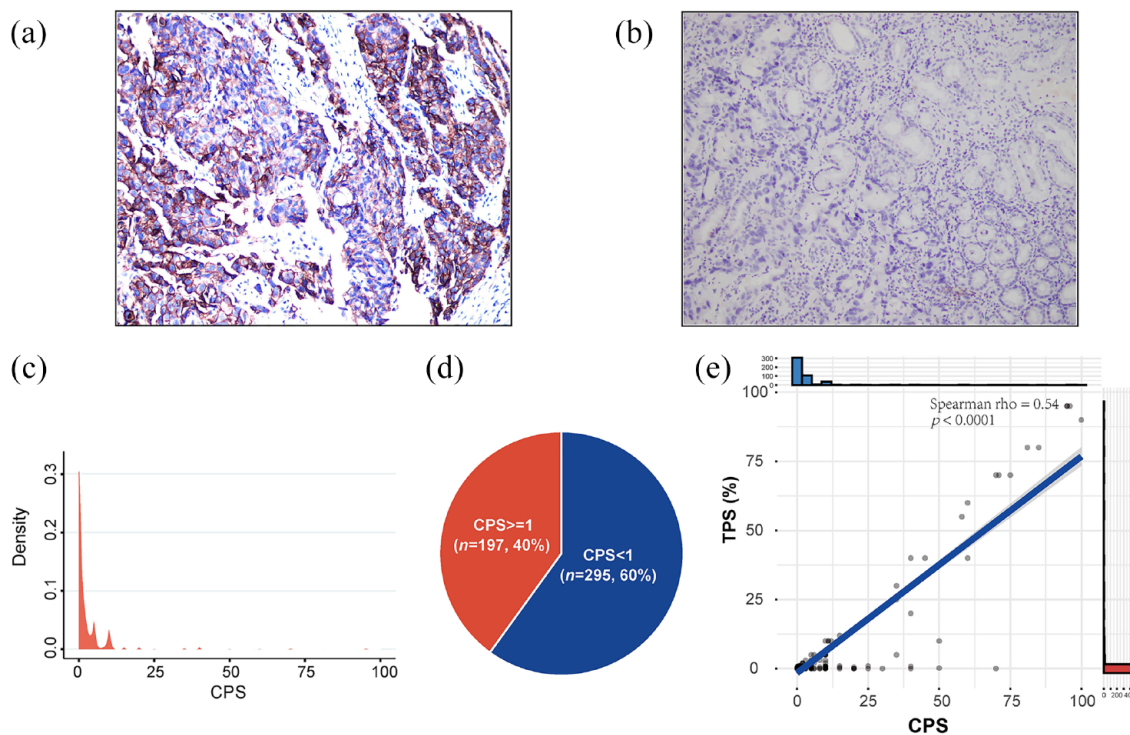


**Figure 1.** PD-L1 expression in PD-L1 positive and PD-L1 negative groups. (a and b) Representative images of PD-L1 expression in PD-L1 positive (a) and PD-L1 negative (b) subjects. (c) Distribution of PD-L1 expression based on the CPS. (d) Distribution of PD-L1 expression [positive ( $\geq 1$ ) and negative ( $< 1$ )] in GC patients. (e) Correlation between the PD-L1 CPS and TPS. CPS, combined positive score; PD-L1, programmed death ligand-1; TPS, tumor percentage score.

0.02 and 1 calculated as  $100 \times \text{median absolute deviation (MAD)}/\text{median of the VAF}$ .<sup>47</sup>

### Pathway analysis

The genes in pathway analysis referred to the previously reported gene list and gene annotation website (<https://reactome.org/>)<sup>48–51</sup> and were compared with the 414 genes covered in the Genecast panel. If an alteration in any gene occurred in a specific pathway, that pathway was considered altered. The final gene list of each pathway is presented in Supplemental Table 3.

### Statistical analysis

Statistical analyses were performed with R software (version 4.0.3; <https://www.r-project.org/>), SPSS software (version 19; <https://www.ibm.com/spss>), and GraphPad Prism software (version 8.0.1; <https://www.graphpad.com/>). Differences between proportions were evaluated by Fisher's exact test. Logistic regression based on the first penalization method was used for multivariate analysis of

categorical variables. The Kruskal–Wallis test was used for comparisons of differences between multiple groups, and post hoc analyses of two matched groups were performed with Dunn's test. For comparison of differences between two groups, the Wilcoxon test was used. Spearman rank correlation coefficients were used to examine correlations. Survival curves were plotted using the Kaplan–Meier analysis, and *p* values were estimated using the log-rank test. All tests were two-sided, and *p* values  $< 0.05$  were considered statistically significant differences unless otherwise stated.

## Results

### Clinical characteristics and PD-L1 expression in the GC cohort

A total of 492 GC patients with both targeted NGS and PD-L1 results were included in the present study. As shown in Figure 1(a) and (b), we evaluated PD-L1 expression using IHC. The median age of all the patients was 62 years (range 19–90). Among the 492 patients, 323 (66%) were

male and 169 (34%) female. The number of all patients with stage I, II, III, and IV disease was 9 (2%), 39 (8%), 152 (31%), and 292 (59%), respectively. MSI-H status was observed in 28 (6%) of the 492 patients. The median CPS of PD-L1 expression was 0.64 [range 1–100; Supplemental Table 2]. The patients were divided into two groups according to the results of the PD-L1 expression assay: a negative PD-L1 expression (PD-L1 negative) group with a CPS < 1 ( $n=295$ , 60%) and a positive PD-L1 expression (PD-L1 positive) group with a CPS  $\geq 1$  [ $n=197$ , 40%; Figure 1(c) and (d)]. The PD-L1 positive patients were older than the PD-L1 negative patients ( $p=0.0039$ ; Supplemental Figure 2). The PD-L1 expression level did not significantly differ by sex gender or clinical stage ( $p>0.05$ ; Supplemental Figure 2).

As another method to evaluate PD-L1 expression, the TPS was applied to assess expression of PD-L1 on tumor cells, and the CPS evaluated expression of PD-L1 in both tumor and immune cells. In this study, the PD-L1 TPS correlated moderately positively with the CPS [Spearman  $\rho=0.54$ ,  $p<0.0001$ ; Figure 1(e)].

#### *Association between summary genomic molecular features and PD-L1 expression status in the GC cohort*

The PD-L1 positive group possessed a higher percentage of MSI-H patients than the PD-L1 negative group [Figure 2(a)]. As a continuous variable, the PD-L1 CPS was modestly associated with an increased TMB [Spearman  $\rho=0.20$ ,  $p<0.0001$ ; Figure 2(b)], and as a categorical variable, the TMB was significantly elevated in PD-L1 positive patients compared to PD-L1 negative patients [ $p<0.001$ ; Figure 2(c)]. However, after excluding MSI-H patients, no significant association was observed between TMB and PD-L1 CPS [ $p=0.054$ ; Figure 2(d)]. PD-L1 CPS showed a weak negative correlation with MATH (Spearman  $\rho=-0.09$ ,  $p=.04$ ) and did not correlate with CNV burden [Spearman  $\rho=0.00421$ ,  $p=0.93$ ; Figure 2(e) and (f)].

#### *Association of individual molecular alterations with PD-L1 expression status in the GC cohort*

We investigated altered genes and pathways that differed between the PD-L1 positive and PD-L1 negative groups. These genomic alterations with

a population percentage greater than 10% (10% included) included *TP53* (64%), *CDH1* (21%), *ARID1A* (18%), *HMCN1* (15%), *KMT2D* (12%), *PIK3CA* (12%), and *KMT2C* [10%; Figure 3(a)]. A total of 40 altered genes were significantly associated with PD-L1 status; 39 genes were more frequently altered in PD-L1 positive cells than in PD-L1 negative cells, including *MSH6* (8% versus 2%), *BCOR* (6% versus 1%), *CTCF* (7% versus 1%), *FLCN* (5% versus 0%), *PIK3CB* (5% versus 0%), *PIK3CA* (16% versus 8%), *KMT2A* (9% versus 3%), *MSH3* (7% versus 2%), *MAP2K4* (6% versus 1%), *ABL1* (5% versus 1%), *WHSC1* (5% versus 1%), and *PDCD1* [3% versus 0%; top 12, all  $p\leq 0.01$ ; Figure 3(b) and Supplemental Table 4]. In contrast, mutations in *CDH1* (15% versus 26%) occurred more commonly in PD-L1 negative samples [ $p<0.01$ ; Figure 3(b) and Supplemental Table 4].

Among the PD-L1 positive and PD-L1 negative groups, there were enrichment diversities of pathway alterations in p53 (65% versus 64%), RTK/RAS (49% versus 46%), DDR (34% versus 32%), SWI/SNF (37% versus 23%), PI3K (37% versus 23%), HMT (31% versus 21%), Notch (17% versus 16%), Wnt (23% versus 14%), TGF $\beta$  (15% versus 13%), cell cycle (14% versus 8%), Hippo (12% versus 6%), HAT (8% versus 6%), KDM (12% versus 5%), Nrf2 (2% versus 2%), DNMT (8% versus 2%), and Myc [3% versus 1%; Figure 3(c)]. In contrast to patients in the PD-L1 negative group, patients in the PD-L1 positive group harbored obvious enrichment (all  $p<0.01$ ) of alterations in PI3K ( $p=0.001$ ), SWI/SNF ( $p=0.001$ ), KDM ( $p=0.003$ ), and DNMT [ $p=0.005$ ; Figure 3(d) and Supplemental Figure 3 A–D].

#### *PD-L1 expression-related PI3K pathway alterations associated with better immunotherapy efficacy*

Based on the findings that genomic pathway alterations in PI3K, SWI/SNF, KDM, and DNMT pathways correlated with PD-L1 expression in the GC cohort, we wondered if these genomic pathway alterations affected the efficacy to ICI treatment in GC patients. Three of the four altered pathways associated with PD-L1 expression identified in the GC cohort, namely, PI3K (62% versus 14%,  $p=0.002$ ), SWI/SNF ( $p=0.038$ ), and KDM ( $p=0.003$ ), had significantly higher alteration rates in the response (R) group than in the nonresponse (NR) group in the SMC immunotherapy cohort<sup>20</sup> [Figure 4(a) and

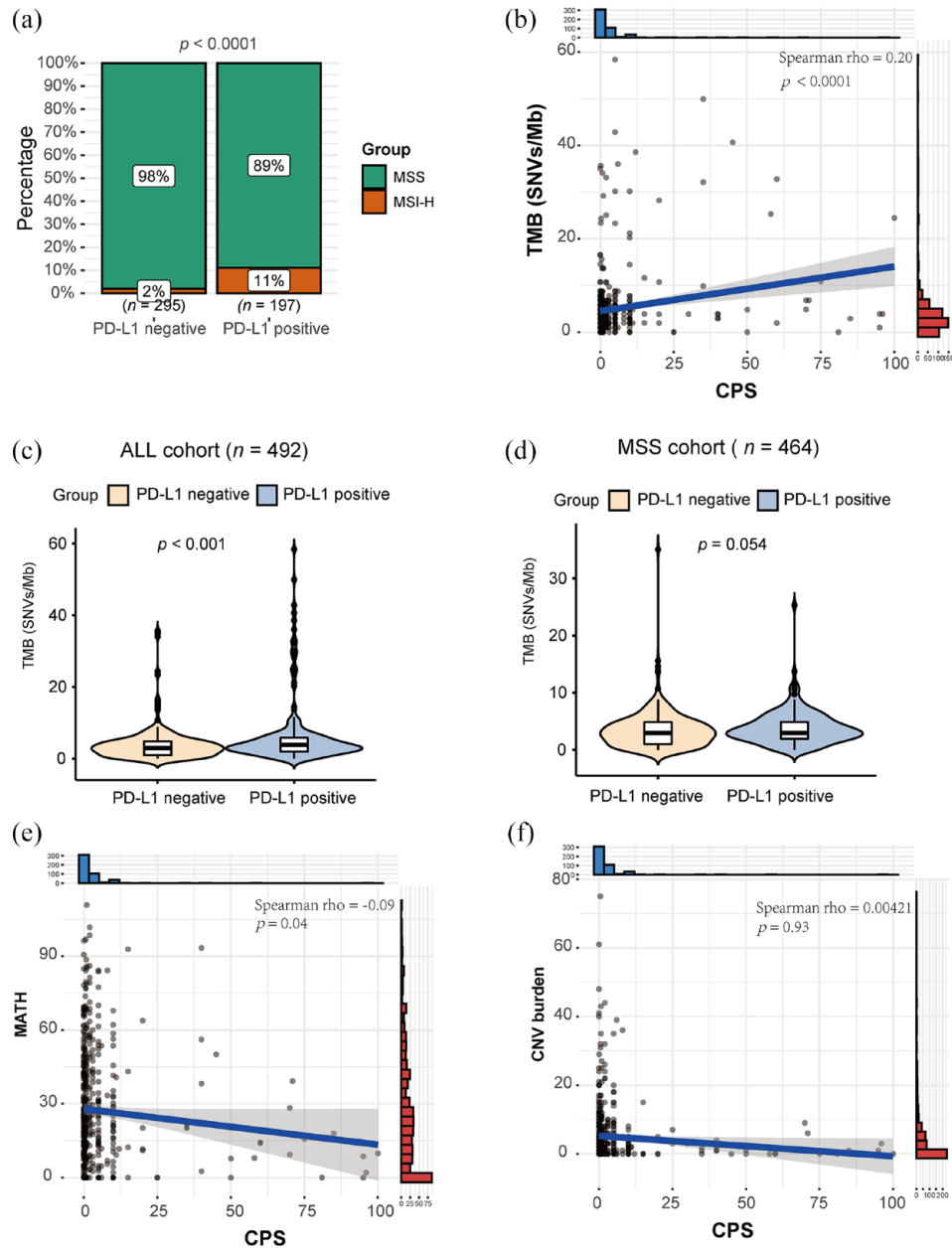


**Figure 2.** Molecular features of PD-L1 expression status in the GC cohort. (a) Comparison of the frequency of MSI status in the PD-L1 positive and PD-L1 negative groups. (b) Correlation between TMB and CPS. (c) Association of TMB and PD-L1 CPS in all GC patients. (d) Association between TMB and PD-L1 CPS in the MSS subgroup of GC patients. (e) Correlation between MATH and CPS. (f) Correlation between the CNV burden and CPS. CNV, copy number variation; CPS, combined positive score; GC, gastric cancer; MATH, mutant-allele tumor heterogeneity; MSI, microsatellite instability; MSS, microsatellite stable; PD-L1, programmed death ligand-1; TMB, tumor mutational burden.

Supplemental Figure 4A]. In addition, no meaningful difference in the alteration rate of the DNMT pathway ( $p = 0.265$ ) was observed between the R and NR groups in the SMC immunotherapy cohort (Supplemental Figure 4A). In the PUCH immunotherapy cohort, the alteration

rate of the PI3K pathway (56% versus 8%,  $p = 0.023$ ) was significantly higher in the DCB group than in the NDB group<sup>21</sup> [Figure 4(b) and Supplemental Figure 4B]. However, there were no significant differences in alteration rates for the other three pathways in the DCB and NDB

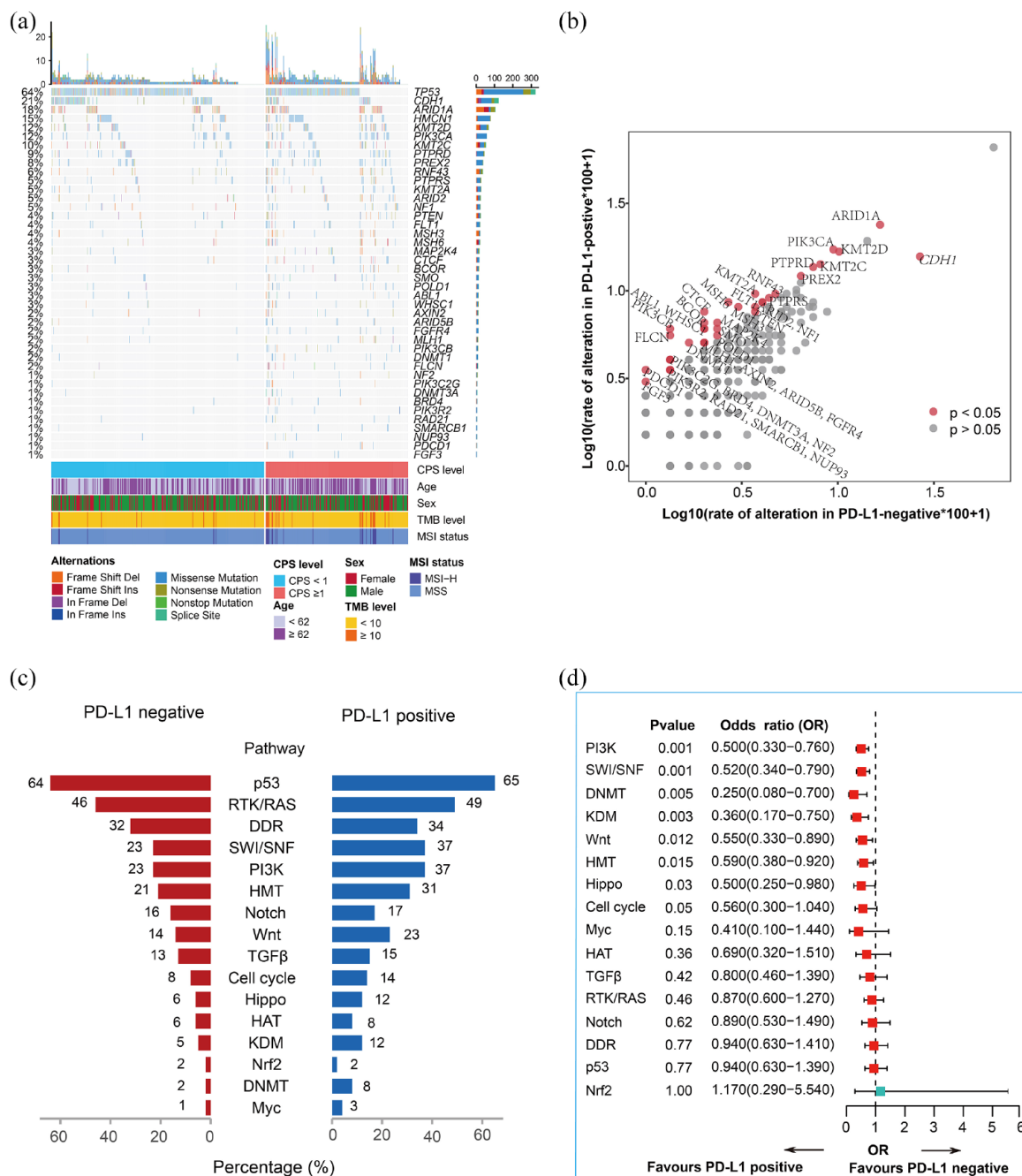


**Figure 3.** Gene and pathway alterations in different PD-L1 expression statuses of the GC cohort. (a) The landscape of gene alterations with population frequencies greater than or equal to 10% and genes with significantly different alteration levels between the PD-L1 positive and PD-L1 negative groups. (b) Distribution of gene alteration rates in the PD-L1 positive group and PD-L1 negative group. The alteration rates of the genes were processed by log<sub>10</sub>. (c) Population percentage of tumors harboring pathway alterations in the PD-L1 positive versus PD-L1 negative groups. (d) Forest plot of comparison results for the frequency of altered pathways in the PD-L1 positive and PD-L1 negative groups. GC, gastric cancer; PD-L1, programmed death ligand-1.

groups (Supplemental Figure 4B). In the MSK immunotherapy cohort containing gastric or gastroesophageal junction adenocarcinomas treated with PD-1 immune checkpoint monotherapy,

pathways with significant differences in alteration rates in the MSK cohort were PI3K (80% versus 21%,  $p=0.038$ ) and SWI/SNF ( $p=0.038$ ), both of which had higher alteration rates in the DCB



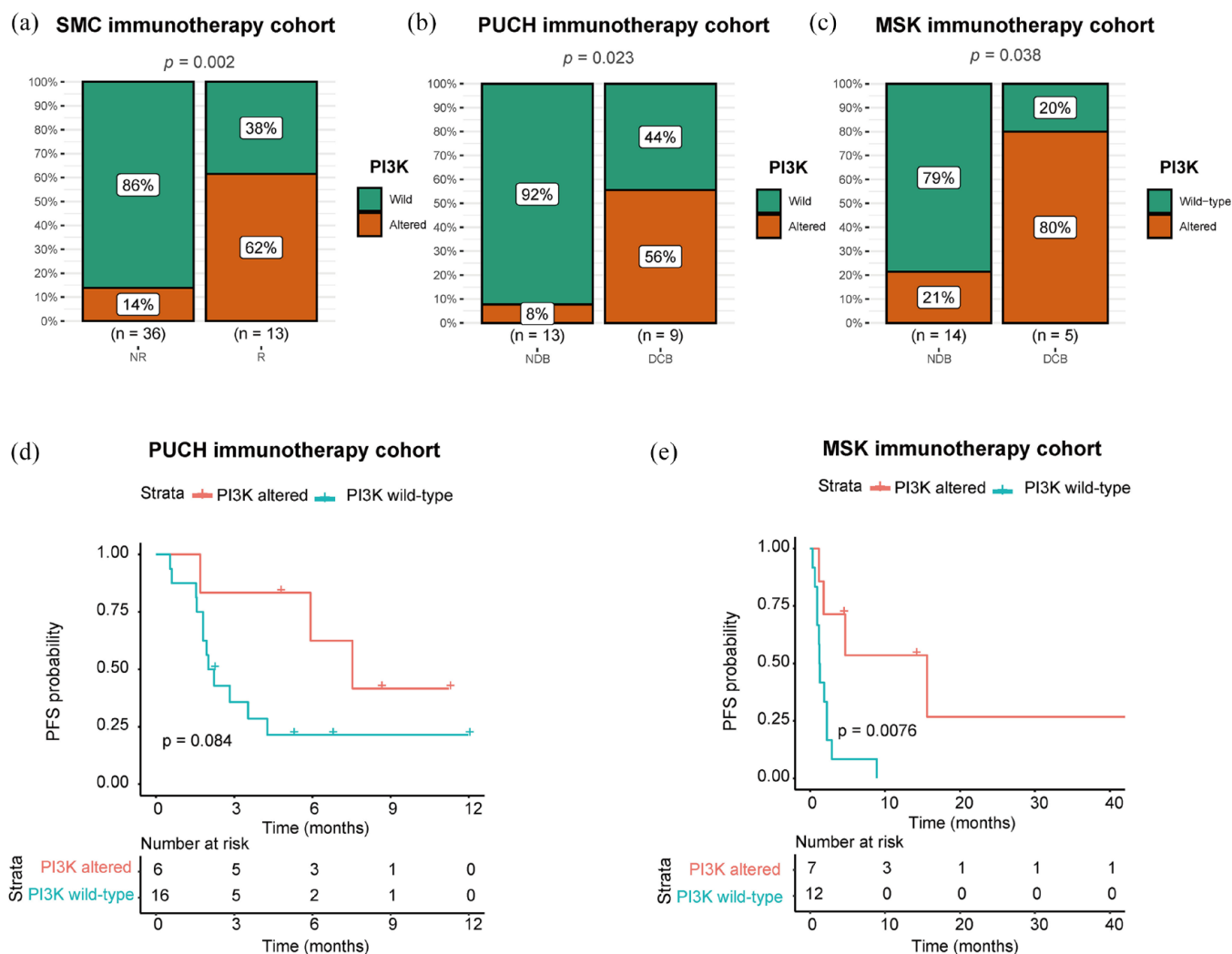


**Figure 4.** Association of PI3K pathway alterations with efficacy and PFS for immunotherapy. (a) Comparison of the frequency of PI3K pathway alterations in the R and NR groups of the SMC immunotherapy cohort. (b) Comparison of the frequency of PI3K pathway alterations in the DCB and NDB groups of the PUCH immunotherapy cohort. (c) Comparison of the frequency of PI3K pathway alterations in the DCB and NDB groups of the MSK immunotherapy cohort. (d) Association of PI3K pathway status with PFS of ICI-treated patients in the PUCH immunotherapy cohort. (e) Association of PI3K pathway status with PFS of ICI-treated patients in the MSK immunotherapy cohort.

DCB, durable clinical benefit; ICI, immune checkpoint inhibitor; MSK, Memorial Sloan Kettering Cancer Center; NDB, no durable benefit; PFS, Progression-free survival; PUCH, Peking University Cancer Hospital; SMC, Samsung Medical Center.

group than in the NDB group [Figure 4(c) and Supplemental Figure 4C]. In summary, PI3K is the common pathway associated with efficacy in the three immunotherapy cohorts.

At the same time, we assessed the correlation between PD-L1 expression and immunotherapy efficacy in both SMC and PUCH immunotherapy cohorts. In the SMC immunotherapy cohort, the PD-L1 positivity rate was significantly higher in the R group than in the NR group (Supplemental Figure 4A). However, in

the PUCH immunotherapy cohort, the difference in PD-L1 positivity rates between the DCB and NDB groups was not significant (Supplemental Figure 4B). Multivariate logistic regression results showed that the PI3K pathway was an independent factor affecting immunotherapy efficacy, whereas PD-L1 expression was not an independent factor in either the SMC or PUCH immunotherapy cohorts (Supplemental Figure 4A and B), suggesting that the PI3K pathway may be more effective for predicting immunotherapy efficacy.

Because PI3K pathway alterations were the only common factor associated with immunotherapy efficacy in the three immunotherapy cohorts, we further explored their relevance to the prognosis of patients treated with ICIs. The Kaplan–Meier analysis suggested that PI3K pathway alterations were significantly associated with longer PFS ( $p=0.0076$ ) in the MSK cohort and showed a certain trend toward significance to be associated with longer PFS ( $p=0.084$ ) in the PUCH cohort [Figure 4(d) and (e)]. For OS, PI3K pathway alterations in the MSK cohort were significantly correlated with longer OS ( $p=0.037$ ), further indicating the potential role of PI3K pathway alteration as a predictor for ICI therapy in GC patients. Meanwhile, PI3K mutation was associated with a trend toward improved OS in PUCH cohort, albeit the correlation was not statistically significant (Supplemental Figure 5A and B).

### Discussion

In clinical practice, it is important to optimize therapy based on the molecular characteristics of tumors in specific populations to improve treatment outcomes and reduce unnecessary toxicity. It has been reported that genetic composition may regulate PD-L1 expression, which in turn affects antitumor immunity.<sup>52</sup> To our knowledge, this is the first study to simultaneously investigate factors associated with PD-L1 expression, including clinical features and genomic molecular features, in Chinese GC patients. Our research indicated that PD-L1 expression correlated not only with the age of GC patients but also with the specific altered pathways of tumors, such as the PI3K pathway. More importantly, PI3K pathway alterations correlated with the efficacy of ICI therapy and the prognosis of ICI-treated patients.

Our data showed that the percentage of PD-L1 positive GC patients ( $CPS \geq 1$ ) was 40% (197/492), which was less than that reported in previous studies (45.9–71.7%).<sup>24,53</sup> This was also noted in the HER2 positive GC cohort, with a PD-L1 positivity rate of 57.3%.<sup>54</sup> This variation across studies may be attributable to a variety of factors, including differences in populations, differences in the cancer stage, prior treatment or the tumor immune microenvironment (TIME) of patients, sample heterogeneity and phenotypic differences, and differences in the PD-L1 antibodies used. Additionally, our results demonstrated that the PD-L1 expression level in older patients was significantly higher than that in younger patients. This was in line with a

previous study,<sup>24</sup> but most studies have not shown a significant difference between PD-L1 expression and age.<sup>54,55</sup> To our knowledge, the present study assessed PD-L1 distribution in the largest GC cohort to date. Further studies on the distribution of PD-L1 expression in different populations are needed to better guide clinical practice.

In GC, there was a correlation between PD-L1 expression, TMB and MSI status. In our study, both the TMB value and proportion of MSI-H patients in the PD-L1 positive group were significantly greater than those in the PD-L1 negative group, but the correlation between TMB and PD-L1 expression disappeared when the MSI-H patients were censored. These results were consistent with a previous gastroesophageal adenocarcinoma (GEA) study involving GC patients<sup>14</sup> and may provide a reason why PD-L1 positive patients are the most likely to benefit from treatment with ICIs.

PI3K pathway alterations may be one of the factors influencing PD-L1 expression and ICI treatment efficacy in GC patients. The phosphatidylinositol 3-kinase (PI3K) signaling pathway affects multiple biological functions of cancer cells, such as cell growth, proliferation, metabolism, and mobility.<sup>56</sup> In colorectal cancer (CRC) and glioma cells, oncogenic activation of the PI3K-AKT pathway can increase PD-L1 expression,<sup>57,58</sup> and this regulation occurs at least partially by altering PD-L1 mRNA levels in melanoma and triple negative breast cancer cells.<sup>52,59,60</sup> In non-small cell lung cancer, oncogenic activation of the AKT–mTOR pathway, which is downstream of the PI3K pathway, has been confirmed to promote immune escape by driving PD-L1 expression in vivo.<sup>61,62</sup> In our study, PI3K pathway alterations were associated with PD-L1 positivity ( $CPS \geq 1$ ) in both the GC cohort and SMC immunotherapy cohort, better efficacy of ICIs in three immunotherapy cohorts (SMC, PUCH, and MSK), longer PFS in ICI-treated GC patients from both the PUCH and MSK immunotherapy cohorts, and longer OS in ICI-treated GC patients from the MSK immunotherapy cohort. The activity of the PI3K–ATK pathway has been associated with antitumor immunity in GC, not only in our study but also in a previous investigation.<sup>63</sup> Nevertheless, a recent study in dMMR/MSI-H gastric adenocarcinoma showed that patients with a high number of mutated genes in the PI3K–AKT–mTOR pathway had a worse objective response rate and shorter PFS

and OS than patients with a low number of mutated genes in the PI3K–AKT–mTOR pathway.<sup>64</sup> We speculate that the reason for this contradiction may be the different subjects of the study, as this previous study included only dMMR/MSI-H patients, which represent a very small fraction of GC patients and may be primitively sensitive to immunotherapy. Our study included both dMMR/MSI-H and pMMR/MSS GC patients. The value of PI3K pathway alterations for predicting response to GC immunotherapy is worthy of further validation in a larger cohort. In addition, some studies have shown that restoration of immune-related signaling, improvement of antigen presentation, increased density of tumor-infiltrating immune cells, and promotion of immune recognition of tumor cells correlate with pharmacological inhibition of the PI3K pathway.<sup>62,65–67</sup> In summary, this may provide a possible explanation for why patients with PI3K pathway alterations benefit more from immunotherapy, strengthening the rationale for combining ICIs with agents targeting the PI3K pathway.

The principal limitations of this study are as follows. First, clinical information, such as prior treatments that may affect the PD-L1 CPS, was not available for the GC cohort. Second, the low number of patients in the validation cohort of immunotherapy may affect the confidence of the results. However, we evaluated the impact of the PD-L1 CPS-related altered pathway on the efficacy of ICIs and prognosis in three separate cohorts, which provides additional evidence to support our findings. Therefore, the relationship of PI3K pathway alterations with the PD-L1 CPS and the efficacy of ICIs and prognosis of ICI-treated patients in a much larger cohort study including both PD-L1 CPS and DNA sequencing data has yet to be validated.

## Conclusion

In conclusion, this is the largest study to date characterizing PD-L1 distribution and the molecular landscape associated with PD-L1 expression in the GC population. Our study highlights that PD-L1 expression status is significantly related to clinical factors and molecular factors. Among them, PI3K pathway alterations are related to PD-L1 positivity and correlate with the efficacy of ICI therapy and the prognosis of ICI-treated patients. Our study provides potential new insights into the use of PI3K pathway alteration status to select more patients who may benefit

from ICI therapy and to develop rational immunotherapy combination strategies for GC patients.

## Declarations

### *Ethics approval and consent to participate*

This study protocol was carried out in accordance with the Declaration of Helsinki and involving human participants and was approved by the Beijing Friendship Hospital, Capital Medical University Ethics Committee (2018-P2-045-01). All the patients participating in the study gave written informed consent before sample collection.

### *Consent for publication*

Not applicable.

### *Author contributions*

**Langbiao Liu:** Conceptualization; Validation; Writing – original draft; Writing – review & editing.

**Lei Niu:** Conceptualization; Validation; Writing – original draft; Writing – review & editing.

**Xue Zheng:** Formal analysis; Validation; Writing – original draft; Writing – review & editing.

**Fei Xiao:** Formal analysis; Validation; Writing – review & editing.

**Huaibo Sun:** Data curation; Validation; Writing – review & editing.

**Wei Deng:** Conceptualization; Supervision; Validation; Writing – review & editing.

**Jun Cai:** Conceptualization; Funding acquisition; Supervision; Validation; Writing – review & editing.

### *Acknowledgements*

None.

### *Funding*

The authors disclosed receipt of the following financial support for the research, authorship, and/or publication of this article: This work was supported by the National Science and Technology Support Program (No. 2015BAI13B09) and National Key R&D Program of China (No. 2017YFC0110904).


### *Competing interests*

XZ, FX, and HS were employed by the company Genecast Biotechnology Co., Ltd. The remaining authors declare no competing interest.

### Availability of data and materials

The datasets underlying this article are available from the corresponding author upon reasonable request.

### ORCID iD

Jun Cai  <https://orcid.org/0000-0003-4254-8843>

### Supplemental material

Supplemental material for this article is available online.

### References

1. Kawazoe A, Yamaguchi K, Yasui H, *et al.* Safety and efficacy of pembrolizumab in combination with S-1 plus oxaliplatin as a first-line treatment in patients with advanced gastric/gastroesophageal junction cancer: Cohort 1 data from the KEYNOTE-659 phase IIb study. *Eur J Cancer* 2020; 129: 97–106.
2. Shitara K, Van Cutsem E, Bang YJ, *et al.* Efficacy and safety of pembrolizumab or pembrolizumab plus chemotherapy vs chemotherapy alone for patients with first-line, advanced gastric cancer: the KEYNOTE-062 phase 3 randomized clinical trial. *JAMA Oncol* 2020; 6: 1571–1580.
3. Janjigian YY, Shitara K, Moehler M, *et al.* First-line nivolumab plus chemotherapy versus chemotherapy alone for advanced gastric, gastro-oesophageal junction, and oesophageal adenocarcinoma (checkmate 649): a randomised, open-label, phase 3 trial. *J Lancet* 2021; 398: 27–40.
4. Kang YK, Boku N, Satoh T, *et al.* Nivolumab in patients with advanced gastric or gastro-oesophageal junction cancer refractory to, or intolerant of, at least two previous chemotherapy regimens (ONO-4538-12, ATTRACTION-2): a randomised, double-blind, placebo-controlled, phase 3 trial. *J Lancet* 2017; 390: 2461–2471.
5. Bang YJ, Ruiz EY, Van Cutsem E, *et al.* Phase III, randomised trial of avelumab versus physician's choice of chemotherapy as third-line treatment of patients with advanced gastric or gastro-oesophageal junction cancer: primary analysis of JAVELIN Gastric 300. *Ann Oncol* 2018; 29: 2052–2060.
6. Fuchs CS, Doi T, Jang RW, *et al.* Safety and efficacy of pembrolizumab monotherapy in patients with previously treated advanced gastric and gastroesophageal junction cancer: phase 2 clinical KEYNOTE-059 trial. *JAMA Oncol* 2018; 4: e180013.
7. Shitara K, Özgüroğlu M, Bang YJ, *et al.* Pembrolizumab versus paclitaxel for previously treated, advanced gastric or gastro-oesophageal junction cancer (KEYNOTE-061): a randomised, open-label, controlled, phase 3 trial. *J Lancet* 2018; 392: 123–133.
8. Moehler M, Dvorkin M, Boku N, *et al.* Phase III trial of avelumab maintenance after first-line induction chemotherapy versus continuation of chemotherapy in patients with gastric cancers: results from JAVELIN Gastric 100. *J Clin Oncol* 2021; 39: 966–977.
9. Muro K, Chung HC, Shankaran V, *et al.* Pembrolizumab for patients with PD-L1-positive advanced gastric cancer (KEYNOTE-012): a multicentre, open-label, phase 1b trial. *Lancet Oncol* 2016; 17: 717–726.
10. Büttner R, Gosney JR, Skov BG, *et al.* Programmed death-Ligand 1 immunohistochemistry testing: a review of analytical assays and clinical implementation in Non-Small-Cell Lung Cancer. *J Clin Oncol* 2017; 35: 3867–3876.
11. Rehman JA, Han G, Carvajal-Hausdorf DE, *et al.* Quantitative and pathologist-read comparison of the heterogeneity of programmed death-ligand 1 (PD-L1) expression in non-small cell lung cancer. *Modern Pathol* 2017; 30: 340–349.
12. Sakakibara R, Inamura K, Tambo Y, *et al.* EBUS-TBNA as a promising method for the evaluation of tumor PD-L1 expression in lung cancer. *Clin Lung Cancer* 2017; 18: 527–534.e1.
13. Rimm DL, Han G, Taube JM, *et al.* A prospective, multi-institutional, pathologist-based assessment of 4 immunohistochemistry assays for PD-L1 expression in Non-Small cell lung cancer. *JAMA Oncol* 2017; 3: 1051–1058.
14. Wang JY, Xiu J, Baca Y, *et al.* Distinct genomic landscapes of gastroesophageal adenocarcinoma depending on PD-L1 expression identify mutations in RAS-MAPK pathway and TP53 as potential predictors of immunotherapy efficacy. *Ann Oncol* 2021; 32: 906–916.
15. Liu X, Choi MG, Kim K, *et al.* High PD-L1 expression in gastric cancer (GC) patients and correlation with molecular features. *Pathol Res Pract* 2020; 216: 152881.
16. Kim YB, Ahn JM, Bae WJ, *et al.* Functional loss of ARID1A is tightly associated with high PD-L1 expression in gastric cancer. *Int J Cancer* 2019; 145: 916–926.
17. Wang J, Xiu J, Baca Y, *et al.* Large-scale analysis of KMT2 mutations defines a distinctive molecular subset with treatment implication in gastric cancer. *Oncogene* 2021; 40: 4894–4905.

18. Wang YL, Gong Y, Lv Z, *et al.* Expression of PD1/PDL1 in gastric cancer at different microsatellite status and its correlation with infiltrating immune cells in the tumor microenvironment. *J Cancer* 2021; 12: 1698–1707.
19. Schoenfeld AJ, Rizvi H, Bandlamudi C, *et al.* Clinical and molecular correlates of PD-L1 expression in patients with lung adenocarcinomas. *Ann Oncol* 2020; 31: 599–608.
20. Kim ST, Cristescu R, Bass AJ, *et al.* Comprehensive molecular characterization of clinical responses to PD-1 inhibition in metastatic gastric cancer. *Nat Med* 2018; 24: 1449–1458.
21. Jiao X, Wei X, Li S, *et al.* A genomic mutation signature predicts the clinical outcomes of immunotherapy and characterizes immunophenotypes in gastrointestinal cancer. *NPJ Precis Oncol* 2021; 5: 36.
22. Janjigian YY, Sanchez-Vega F and Jonsson P. Genetic predictors of response to systemic therapy in esophagogastric cancer. *Cancer Discov* 2018; 8: 49–58.
23. Bang YJ, Kang YK, Catenacci DV, *et al.* Pembrolizumab alone or in combination with chemotherapy as first-line therapy for patients with advanced gastric or gastroesophageal junction adenocarcinoma: results from the phase II nonrandomized KEYNOTE-059 study. *Gastric Cancer* 2019; 22: 828–837.
24. Yamashita K, Iwatsuki M, Harada K, *et al.* Prognostic impacts of the combined positive score and the tumor proportion score for programmed death ligand-1 expression by double immunohistochemical staining in patients with advanced gastric cancer. *Gastric Cancer* 2020; 23: 95–104.
25. Wang K, Li M and Hakonarson H. ANNOVAR: functional annotation of genetic variants from high-throughput sequencing data. *Nucleic Acids Res* 2010; 38: e164.
26. Sherry ST, Ward MH, Kholodov M, *et al.* dbSNP: the NCBI database of genetic variation. *Nucleic Acids Res* 2001; 29: 308–311.
27. Abecasis GR, Auton A, Brooks LD, *et al.* An integrated map of genetic variation from 1,092 human genomes. *Our Nat* 2012; 491: 56–65.
28. Karczewski KJ, Weisburd B, Thomas B, *et al.* The ExAC browser: displaying reference data information from over 60 000 exomes. *Nucleic Acids Res* 2017; 45: D840–d845.
29. Liu X, Jian X and Boerwinkle E. dbNSFP: a lightweight database of human nonsynonymous SNPs and their functional predictions. *Hum Mutat* 2011; 32: 894–899.
30. Forbes SA, Bindal N, Bamford S, *et al.* COSMIC: mining complete cancer genomes in the catalogue of somatic mutations in cancer. *Nucleic Acids Res* 2011; 39: D945–D950.
31. Koboldt DC, Zhang Q, Larson DE, *et al.* VarScan 2: somatic mutation and copy number alteration discovery in cancer by exome sequencing. *Genome Res* 2012; 22: 568–576.
32. Talevich E, Shain AH, Botton T, *et al.* CNVkit: genome-wide copy number detection and visualization from targeted DNA sequencing. *PLoS Comput Biol* 2016; 12: e1004873.
33. Chen S, Zhou Y, Chen Y, *et al.* fastp: an ultra-fast all-in-one FASTQ preprocessor. *Bioinformatics (Oxford, England)* 2018; 34: i884–i890.
34. Cibulskis K, Lawrence MS, Carter SL, *et al.* Sensitive detection of somatic point mutations in impure and heterogeneous cancer samples. *Nat Biotechnol* 2013; 31: 213–219.
35. McLaren W, Gil L, Hunt SE, *et al.* The Ensembl variant effect predictor. *Genome Biol* 2016; 17: 122.
36. Ng PC and Henikoff S. SIFT: predicting amino acid changes that affect protein function. *Nucleic Acids Res* 2003; 31: 3812–3814.
37. Adzhubei I, Jordan DM and Sunyaev SR. Predicting functional effect of human missense mutations using PolyPhen-2. *Curr Protoc Human Genet* 2013; Chapter 7: Unit7.20.
38. Duval A and Hamelin R. Mutations at coding repeat sequences in mismatch repair-deficient human cancers: toward a new concept of target genes for instability. *Cancer Res* 2002; 62: 2447–2454.
39. Zhu L, Huang Y, Fang X, *et al.* A novel and reliable method to detect microsatellite instability in colorectal cancer by next-generation sequencing. *J Mol Diagn* 2018; 20: 225–231.
40. Nowak JA, Yurgelun MB, Bruce JL, *et al.* Detection of mismatch repair deficiency and microsatellite instability in colorectal adenocarcinoma by targeted next-generation sequencing. *J Mol Diagn* 2017; 19: 84–91.
41. Stadler ZK, Battaglin F, Middha S, *et al.* Reliable detection of mismatch repair deficiency in colorectal cancers using mutational load in next-generation sequencing panels. *J Clin Oncol* 2016; 34: 2141–2147.
42. Ready N, Hellmann MD, Awad MM, *et al.* First-line nivolumab plus ipilimumab in advanced Non-Small-Cell lung cancer (checkmate 568): outcomes by programmed death ligand 1 and

- tumor mutational burden as biomarkers. *J Clin Oncol* 2019; 37: 992–1000.
43. Samstein RM, Lee CH, Shoushtari AN, *et al.* Tumor mutational load predicts survival after immunotherapy across multiple cancer types. *Nat Genet* 2019; 51: 202–206.
  44. Chalmers ZR, Connelly CF, Fabrizio D, *et al.* Analysis of 100,000 human cancer genomes reveals the landscape of tumor mutational burden. *Genome Med* 2017; 9: 34.
  45. Klemptner SJ, Fabrizio D, Bane S, *et al.* Tumor mutational burden as a predictive biomarker for response to immune checkpoint inhibitors: a review of current evidence. *Oncologist* 2020; 25: e147–e159.
  46. Mroz EA and Rocco JW. MATH, a novel measure of intratumor genetic heterogeneity, is high in poor-outcome classes of head and neck squamous cell carcinoma. *Oral Oncol* 2013; 49: 211–215.
  47. Mroz EA, Tward AD, Hammon RJ, *et al.* Intra-tumor genetic heterogeneity and mortality in head and neck cancer: analysis of data from the Cancer Genome Atlas. *PLoS Med* 2015; 12: e1001786.
  48. Sanchez-Vega F, Mina M and Armenia J. Oncogenic signaling pathways in the cancer genome atlas. *Cell* 2018; 173: 321–337.e310.
  49. Miao D, Margolis CA, Gao W, *et al.* Genomic correlates of response to immune checkpoint therapies in clear cell renal cell carcinoma. *Science* 2018; 359: 801–806.
  50. Knijnenburg TA, Wang L and Zimmermann MT. Genomic and molecular landscape of DNA damage repair deficiency across the cancer genome atlas. *Cell Rep* 2018; 23: 239–254.e236.
  51. Cheng X and Blumenthal RM. Mammalian DNA methyltransferases: a structural perspective. *Structure (London, England 1993)* 2008; 16: 341–350.
  52. Cha JH, Chan LC, Li CW, *et al.* Mechanisms controlling PD-L1 expression in cancer. *Mol Cell* 2019; 76: 359–370.
  53. Ibbes M, Miller M and Hadjipanayis A. Comprehensive molecular characterization of gastric adenocarcinoma. *Nature* 2014; 513: 202–209.
  54. Lian J, Zhang G, Zhang Y, *et al.* PD-L1 and HER2 expression in gastric adenocarcinoma and their prognostic significance. *Digest Liver Dis* 2022; 54(10): 1419–1427.
  55. Zhang M, Dong Y, Liu H, *et al.* The clinicopathological and prognostic significance of PD-L1 expression in gastric cancer: a meta-analysis of 10 studies with 1,901 patients. *Sci Rep* 2016; 6: 37933.
  56. Sun C, Mezzadra R and Schumacher TN. Regulation and function of the PD-L1 checkpoint. *Immunity* 2018; 48: 434–452.
  57. Song M, Chen D, Lu B, *et al.* PTEN loss increases PD-L1 protein expression and affects the correlation between PD-L1 expression and clinical parameters in colorectal cancer. *PLoS One* 2013; 8: e65821.
  58. Parsa AT, Waldron JS, Panner A, *et al.* Loss of tumor suppressor PTEN function increases B7-H1 expression and immunoresistance in glioma. *Nat Med* 2007; 13: 84–88.
  59. Jiang X, Zhou J, Giobbie-Hurder A, *et al.* The activation of MAPK in melanoma cells resistant to BRAF inhibition promotes PD-L1 expression that is reversible by MEK and PI3K inhibition. *Clin Cancer Res* 2013; 19: 598–609.
  60. Mittendorf EA, Philips AV, Meric-Bernstam F, *et al.* PD-L1 expression in triple-negative breast cancer. *Cancer Immunol Res* 2014; 2: 361–370.
  61. Lastwika KJ, Wilson W 3rd, Li QK, *et al.* Control of PD-L1 expression by oncogenic activation of the AKT-mTOR pathway in non-small cell lung cancer. *Cancer Res* 2016; 76: 227–238.
  62. O'Donnell JS, Massi D, Teng MWL, *et al.* PI3K-AKT-mTOR inhibition in cancer immunotherapy, redux. *Semin Cancer Biol* 2018; 48: 91–103.
  63. He Y and Wang X. Identification of molecular features correlating with tumor immunity in gastric cancer by multi-omics data analysis. *Ann Transl Med* 2020; 8: 1050.
  64. Wang Z, Wang X, Xu Y, *et al.* Mutations of PI3K-AKT-mTOR pathway as predictors for immune cell infiltration and immunotherapy efficacy in dmmr/MSI-H gastric adenocarcinoma. *BMC Med* 2022; 20: 133.
  65. Marijt KA, Sluiter M, Blijleven L, *et al.* Metabolic stress in cancer cells induces immune escape through a PI3K-dependent blockade of IFN $\gamma$  receptor signaling. *J Immunother Cancer* 2019; 7: 152.
  66. Sai J, Owens P, Novitskiy SV, *et al.* PI3K inhibition reduces mammary tumor growth and facilitates antitumor immunity and anti-PD1 responses. *Clin Cancer Res* 2017; 23: 3371–3384.
  67. Borcoman E, De La Rochere P, Richer W, *et al.* Inhibition of PI3K pathway increases immune infiltrate in muscle-invasive bladder cancer. *Oncoimmunology* 2019; 8: e1581556.